Hygroscopic Power Generation Performance of a New Type of Lithium-Ion Battery Material Based on Lithium Chloride-modified Delignified Wood and Far-Infrared Paper

Zheyu Li,[#] Wei Zhao,[#] Zhihong Zhao,[#] Wenjing Liu, Yipeng Huang, Yupeng Wu, and Minghui Zhang,*

With the growing global demand for sustainable energy, the development of efficient and environmentally friendly energy conversion and storage materials has become a research hotspot. Paulownia wood, with its natural porous structure and good hygroscopicity, is considered a highly promising biomass material. However, its properties still need to be further optimized through pretreatment to meet specific application requirements. In this study, paulownia wood was chemically modified through delignification and lithium chloride (LiCl) compounding, and far-infrared paper was attached to its surface to enhance its hygroscopicity and electrochemical performance. These pretreatment methods not only increased the porosity of paulownia wood, but also significantly improved the ion transport capacity, thereby achieving excellent moisture absorption and power generation performance in a high humidity environment. Experimental results showed that the LiCl and delignified paulownia composite materials (DW@LiCl) material exhibited excellent electrochemical performance during the hygroscopic process: its current continuously increased with humidity, and the final voltage reached 0.494 V, which was significantly higher than that of other control groups. This modified paulownia wood material demonstrated significant application value in the field of hygroscopic power generation, such as directly generating electricity from ambient humidity, and it exhibits potential for the development of high-performance lithium-ion batteries.

DOI: 10.15376/biores.20.2.3415-3423

Keywords: Hygroscopic; Delignification; Wood power generation; Moisture content

*Contact information: College of Materials Science and Art Design, Inner Mongolia Agricultural University, Hohhot 010018, Inner Mongolia, China; #These authors contributed equally to this work; *Corresponding author: zhangminghui@imau.edu.cn*

INTRODUCTION

With the continuous growth of global energy demand and the increasing severity of environmental issues, the development of sustainable energy technologies has become particularly urgent (Duan *et al.* 2025). Water vapor in the air, a ubiquitous yet underutilized potential energy source, is gaining increasing attention due to its significant potential for energy conversion (Edström and Dahlbäck 2024). In recent years, hygroscopic electricity generation technology has emerged as a new method of energy conversion. This technology generates electricity through the migration of moisture in response to environmental humidity, providing a new direction for the development of sustainable energy (Nguyen *et al.* 2024). For example, Hu *et al.* (2024) has proposed a cyclic hygro-

evaporative power fabric (Mac-fabric), an asymmetric fabric that uses a capillary effect to absorb water on one side and efficiently expel it from the other, and the directional movement of these ions increases the ion current density, resulting in a sustainable high-performance output. In the study of hygroscopic electricity generation, the porosity and hygroscopicity of materials are key factors affecting their performance (Wang *et al.* 2024). Materials with high porosity can provide more channels for moisture migration, thereby improving transmission efficiency, while good hygroscopicity enables materials to quickly absorb moisture in high-humidity environments, thus enhancing the efficiency of electricity generation (Huang *et al.* 2025; Liu *et al.* 2025). Wood, with its natural porous structure and good hygroscopicity, has become an ideal candidate material (Zhang *et al.* 2024). Studies have found that delignification treatment can further increase the porosity and hygroscopicity of wood, making delignification an important step in the preparation of hygroscopic wood (Chen *et al.* 2024; Li *et al.* 2025). The natural ion wood generator developed by Li *et al.* (2022) is based on the preparation of lignin-removed wood, which is then subjected to *in situ* composite formation with hydrogel and lithium chloride (LiCl). This process results in the formation of a spider-web-like LiCl salt structure on the inner walls of the microchannels within the wood. This unique structure enables the conversion of ambient moisture into electrical energy (Li *et al.* 2022).

In addition, LiCl, as an electrolyte, can improve the conductivity and ion transport efficiency of materials when compounded with them (Tang *et al.* 2024). It has also been found that attaching far-infrared paper to the surface of wood can significantly enhance the electrical properties of the wood. Far-infrared paper, with its excellent far-infrared emission properties, can emit far-infrared electromagnetic waves of specific wavelengths when attached to the wood surface. These far-infrared waves promote ion migration and charge distribution within the wood, thereby enhancing its conductivity (Shi *et al.* 2025). This synergistic effect enables the wood to exhibit higher current and voltage during hygroscopic electricity generation, thus significantly improving its energy conversion efficiency.

In this study, a novel delignified aerogel wood was successfully prepared. Using this aerogel wood as a base, an ionic wood was developed through the synergistic action of LiCl freezing and salting-out. By attaching far-infrared paper to the surface of the ionic wood, a movable ion concentration gradient was formed, enabling hygroscopic electricity generation. This material not only performed excellently in hygroscopic electricity generation, but the work also provides new ideas and solutions for the development of high-performance lithium-ion batteries.

EXPERIMENTAL

Materials

Paulownia (Natural wood, NW) was sourced from Hebei Province, China, ensuring the selection of materials free from mold and obvious defects.

Anhydrous ethanol (Tianjin Xinbote Chemical Co., Ltd.), sodium chlorite (Shanghai Maclin Biochemical Technology Co., Ltd.), glacial acetic acid (Tianjin Xinbote Chemical Co., Ltd.), anhydrous LiCl (Shandong Keyuan Biochemical Co., Ltd.), and anhydrous sodium acetate (Tianjin Xinbote Chemical Co., Ltd.) were used as received. The distilled water used for experiments was prepared in the laboratory.

Preparation of Wood-based Power Generation Materials

Pre-conditioning

1. Raw Materials and Treatment: Small sections of paulownia wood were cut into blocks of dimensions (30 (T) × 30 (R) × 10 (L) mm^3). Several pieces of sapwood were selected and kept them in a forced-air drying oven at 103± 2°C until they reached an oven-dry state. The oven-dry mass of the wood was recorded as m_0.

2. Preparation of Delignification Reagent: About 0.2 mol/L of sodium acetate (NaAc) was mixed with 0.2 mol/L acetic acid (HAc), the pH of the buffer solution was adjusted to approximately 4.6± 0.2. Then a 5 wt% of sodium chlorite ($NaClO_2$) solution was added to the buffer solution to prepare the delignification solution.

3. Preparation of Lithium Chloride Solution: 200 mL 10 wt% LiCl solution was prepared.

Preparation of delignified wood (DW)

The oven-dried paulownia wood was added into a beaker containing the delignification solution and heated in a constant temperature water bath at 95 ± 2 °C for 24 h. Then, the wood was soaked in distilled water; the water was changed every 2 h.

During this washing process, a pH paper was used to test the acidity of the waste liquid until the pH value of the waste liquid was approximately 7, indicating that the residual acid within the specimens had been nearly completely removed. After that, the specimens were soaked in anhydrous ethanol for 12 h to obtain the delignified wood (DW). This was then dried in a freeze dryer for 12 h. Finally, the specimens were weighed using a balance to obtain m_1.

Preparation of LiCl and paulownia composite materials (NW@LiCl)

The procedure was to immerse the completely dry NW in 100 mL 10 wt% LiCl solution for 1 hour so that LiCl was fully loaded by NW. NW was then removed from the LiCl solution and dried in a freeze-dryer to prepare NW@LiCl composites.

Preparation of LiCl and delignified paulownia composite materials (DW@ LiCl)

The completely dry DW was immersed in 100 mL of 10 wt% LiCl solution for 1 hour so that LiCl was fully loaded by DW. DW was then removed from the LiCl solution and dried in a freeze-dryer to prepare DW@LiCl composites.

Characterization of electrical properties and water uptake

Four materials (NW, DW, NW@LiCl, and DW@LiCl) were placed in a constant temperature and humidity chamber at 25± 2 °C and 80±5% relative humidity (RH). The mass changes of these materials were measured at hourly intervals to determine the variations in their water absorption extents.

Simultaneously, every hour, the cross-sectional ends of the wood samples were wrapped with far-infrared paper. A multimeter was used to measure the changes in current and voltage across the cross-sectional ends of the four materials by placing its positive and negative electrodes on the infrared paper at both ends of the wood samples.

RESULTS AND DISCUSSION

Measurement of Mass Loss Extent of DW

To increase the porosity of the wood, this study initially conducted a delignification treatment on the wood. Research indicates that acidic treatment can enlarge the pores of wood (Zhou *et al.* 2024). Table 1 shows the mass loss extent of three NW specimens after delignification. The purpose of using three NW specimens was to reduce the effects of experimental errors. The results showed a mass loss extent (P_1) of 53.01% ± 2%. After the delignification treatment, the material's surface color changed into white, as the color of the wood is primarily derived from the chromophores in lignin (Zhang *et al.* 2023). This is shown in Fig. 1. The change in color indicates that the lignin was effectively removed after the delignification treatment, and the significant increase in the mass loss extent further confirms this point.

Table 1. Mass Loss Extent

Test Specimen	M_0 (g)	M_1 (g)	P_1 (%)
1	2.704	1.202	55.55
2	3.778	1.807	52.17
3	2.686	1.308	51.30
Mean value			53.01

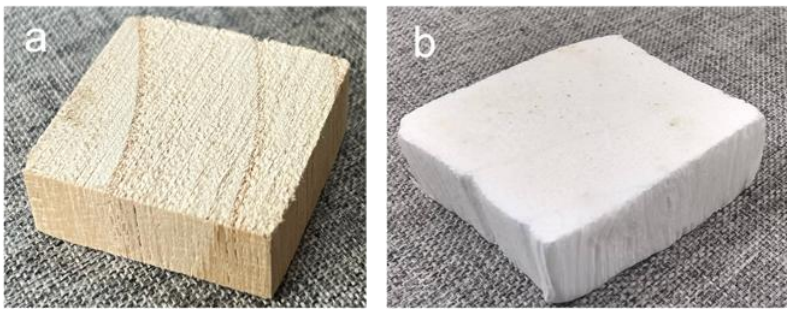

Fig. 1. (a) NW Digital photograph; (b) DW Digital photograph

Hygroscopic Properties of Wood

Figure 2a displays the moisture adsorption curves of NW, DW, NW@LiCl, and DW@LiCl under conditions of 25 °C and 80% RH, while Fig. 2b shows the derivatives of these curves, representing the changes in the extent of moisture absorption. It can be observed from the figures that the moisture absorption curves of NW and DW had a smaller slope from 0 to 1.0 h, indicating a slower extent of moisture absorption. In contrast, the moisture absorption curves of NW@LiCl and DW@LiCl exhibited larger slopes during the same period. As the moisture adsorption process continued, the slope of DW@LiCl's moisture adsorption curve gradually decreased after 1 h, eventually approaching zero. The moisture adsorption extents of the other three materials also gradually decreased and eventually stabilized, reaching an equilibrium state at 13 h. The equilibrium moisture adsorption of NW was 0.110 g/g, that of DW was 0.122 g/g, and that of NW@LiCl was 0.316 g/g. Specimen DW@LiCl had the highest equilibrium moisture absorption, reaching 1.074 g/g. The main reason for this difference lies in the hydrophobic nature of lignin; after delignification treatment, this hydrophobicity is reduced, thereby enhancing the material's moisture absorption capability. Additionally, the presence of LiCl may also affect the

moisture absorption performance of the samples. As shown in Fig 2a, the hygroscopicity of the material was significantly increased compared to that of NW and DW after the incorporation of LiCl. This is because LiCl is a hygroscopic salt and a strong electrolyte. The small ionic radius and high charge density of Li^+ ions enable them to strongly attract water molecules from the air, forming stable lithium hydrate ions (Bunpheng *et al.* 2025).

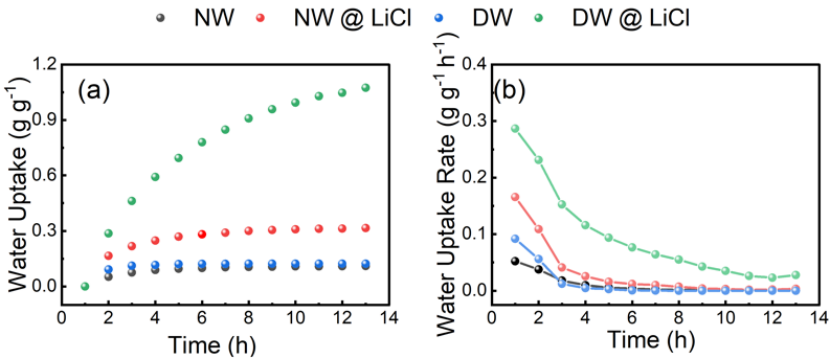

Fig. 2. (a) The change of water absorption of different materials with time; and (b) Moisture absorption extent curve

Analysis of Electrical Properties of Composite Materials

Figure 3a shows the electrical current variations of NW, DW, NW@LiCl, and DW@LiCl over 13 h in a constant temperature and humidity chamber. The observations indicate that the current of NW and DW remained at zero throughout the 13 h, which can be attributed to their minimal moisture absorption and the lack of mobile ions within the samples, which prevented the electrical current from increasing with the rising moisture content. In contrast, the current of NW@LiCl and DW@LiCl exhibited an upward trend during the period of 0 to 5 h, indicating that as the internal moisture increased, the mobility of the ions was enhanced, leading to a gradual increase in current. However, starting from the 6th hour, the current trends of the two materials diverged. Specifically, the NW@LiCl, which had not undergone delignification, reached a dynamic equilibrium in moisture absorption, hindering the directional movement of chloride and lithium ions within the material. The surface moisture could not further penetrate the material, causing the accumulation and loss of chloride and lithium ions at the surface, which led to a decrease in electrical current. In contrast, the current of DW@LiCl continued to increase with the rising moisture content, likely because the delignification treatment increased porosity. facilitating the penetration and movement of moisture and ions, thereby enhancing the material's electrical conductivity.

Figure 3b illustrates the voltage changes of NW, DW, NW@LiCl, and DW@LiCl over 13 h. The voltage of NW remained constant at 0V throughout the experiment. The voltage variation of DW exhibited three stages: from 1 to 4 h, the voltage gradually increased; from 4 to 8 h, the curve flattened out; and from 8 to 13 h, the slope initially increased and then decreased, ultimately reaching a stable state. The voltage changes of NW@LiCl and DW@LiCl showed a rapid increase in slope during the first 1 to 2 h, followed by a nearly constant slope from 2 to 12 h, with an overall trend of gradual increase in voltage. The samples under different treatment conditions displayed varying voltage responses: NW consistently maintained a voltage of 0V; the voltages of NW@LiCl and DW@LiCl eventually approached each other, with DW@LiCl being slightly higher than NW@LiCl; while the voltage of DW, which had not been treated with LiCl solution,

showed a significant difference compared to the first two. These voltage changes may be attributed to the increase in average moisture content of the samples, leading to higher water content. The evaporation extent of moisture was proportional to the moisture content, thereby facilitating the movement of moisture within the samples and generating voltage. Within a certain range, the higher the moisture content, the more ions were oriented to move within the samples, correspondingly resulting in a higher voltage value.

Figure 3c illustrates the resistance changes of NW, DW, NW@LiCl, and DW@LiCl over a period of 13 h. At the initial stage, the resistance of all specimens was infinite, indicating a lack of conductive medium within the materials. However, after 1 h of hygroscopic treatment, the resistance values of NW@LiCl and DW@LiCl dropped significantly, which can be attributed to the addition of moisture effectively reducing the specimens' resistance. Starting from the 2nd hour, the resistance curves of NW@LiCl and DW@LiCl generally showed an increasing trend. This trend is due to the further absorbed moisture leading to a dilution of the LiCl solution, which in turn increases the number of ionized chloride and lithium ions, causing the resistance value to increase. As the moisture content in the specimens increased, the LiCl solution originally dissolved in the specimens was diluted, leading to a decrease in its concentration. Lithium chloride, as an electrolyte, can ionize into chloride and lithium ions in an aqueous solution. The increase in these ions enhances the conductivity within the material, thereby reducing the resistance value. As the hygroscopic process continued, moisture further penetrated the material, further diluting the LiCl solution and increasing the resistance value. This process reveals the electrical behavior of wood-based composite materials under different environmental humidity conditions. To gain a deeper understanding of these phenomena, future studies can further explore the impact of LiCl concentration, treatment time, and environmental humidity on the resistance of wood-based composite materials.

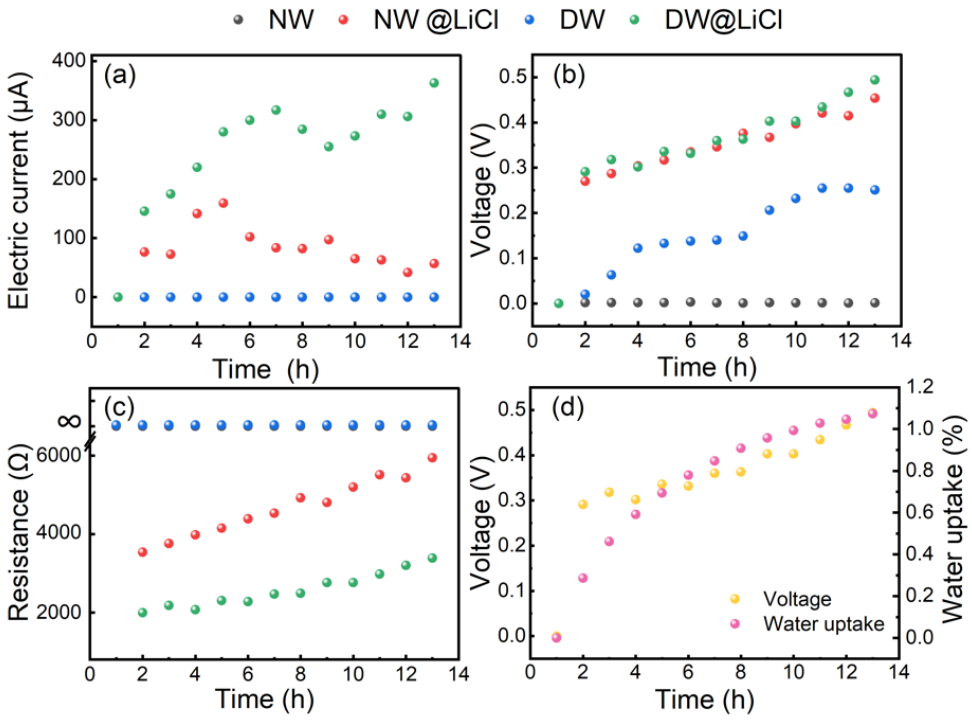

Fig. 3. (a) Electric current change diagram; (b) Voltage variation diagram; (c) Resistance change diagram; and (d) Voltage water content curve

As shown in Fig. 3d, the voltage of DW@LiCl increased significantly with the increase of moisture content, revealing a positive correlation between moisture content and voltage. This relationship can be attributed to the enhanced ionization degree of LiCl after absorbing moisture, leading to an increase in conductivity. As the moisture content increases, the ionization of the LiCl solution generates more Li^+ and Cl^- ions, which provide more charge carriers within the material, thereby enhancing its electrical conductivity. Additionally, the increase in moisture content may also be related to changes in the surface structure and composition of the material, which further affect the material's electrical properties. The electrical behavior of DW@LiCl under varying environmental humidity indicates that the resistivity of wood-based composite material is significantly affected by hygroscopic behavior, a finding of great importance for understanding the performance of materials under different environmental conditions.

CONCLUSIONS

1. In this study, through a specific treatment process, the average delignification extent of paulownia wood reached 53.0%, significantly enhancing the material's hygroscopicity and porosity. Among them, under 80% relative humidity conditions, the DW@LiCl composite material exhibited the highest hygroscopicity, reaching 1.07 g/g.
2. In terms of electrical current response, within 0 to 13 h, the current of the DW@LiCl composite material increased with the rise in moisture content, while after 5 h, the current of the NW@LiCl composite material decreased with the increase in moisture content.
3. Regarding voltage characteristics, the DW@LiCl composite material, NW@LiCl composite material, and DW all showed an upward trend, with final voltages of 0.494V, 0.454V, and 0.251V, respectively, while the voltage of NW was only 0.001V.
4. In terms of resistance, the initial resistance of all materials was infinitely high, but as the hygroscopic process proceeded, the concentration of LiCl in the DW@LiCl composite material and NW@LiCl composite material decreased, leading to an increase in resistance.
5. In summary, this study emphasizes the great potential of high-performance lithium-ion batteries constructed from delignified paulownia wood in combination with lithium chloride and far-infrared paper in sustainable energy production. The materials reported in this study are expected to be strong candidates for high-performance lithium-ion batteries and provide new ideas for the development of sustainable energy technologies.

ACKNOWLEDGMENTS

This work was supported by the Natural Science Foundation of Inner Mongolia Autonomous Region of China (2023MS03027). National Natural Science Foundation of China (31860185 and 31160141), the Research Fund for Introducing high-level Talents in

public institutions of the Autonomous Region in 2022 (DC2300001283), and the Research Start-up Project for Introducing high-level Outstanding Doctoral Talents of Inner Mongolia Agricultural University (NDYB2022-35).

REFERENCES CITED

Bunpheng, A., Chavalekvirat, P., Tangthana-umrung, K., Deerattrakul, V., Nueangnoraj, K., Hirunpinyopas, W., and Iamprasertkun, P. (2025). "A comprehensive study of affordable 'water-in-salt' electrolytes and their properties," *Green Chemical Engineering* 6, 126-135. DOI: 10.1016/j.gce.2024.06.004

Chen, C., Shen, L., Sun, Y., Bao, L., and Wang, X. (2024). "Densification of fast-growing paulownia wood for tough composites with stab resistance," *Cellulose* 31, 3843-3853. DOI: 10.1007/s10570-024-05812-0

Duan, P., Wang, C., Huang, Y., Fu, C., Lu, X., Zhang, Y., Yao, Y., Chen, L., He, Q.-C., Qian, L., and Yang, T. (2025). "Moisture-based green energy harvesting over 600 hours via photocatalysis-enhanced hydrovoltaic effect," *Nature Communications* 16, article 239. DOI: 10.1038/s41467-024-55516-z

Edström, F., and Dahlbäck, P. (2024). "Atmospheric water vapour as a potential water source and its impact on energy systems," *Nature Reviews Materials* 9, 671-672. DOI: 10.1038/s41578-024-00727-5

Hu, Y., Yang, W., Wei, W., Sun, Z., Wu, B., Li, K., Li, Y., Zhang, Q., Xiao, R., Hou, C., and Wang, H. (2024). "Phyto-inspired sustainable and high-performance fabric generators via moisture absorption-evaporation cycles," *Science Advances* 10, article 4620. DOI: 10.1126/sciadv.adk4620

Huang, G., Liu, J., Zhang, H., Zhang, W., Deng, Y., and Sha, J. (2025). "A double-gradient structured hydrogel for an efficient moisture-electric generator," *Chemical Engineering Journal* 504, article 158878. DOI: 10.1016/j.cej.2024.158878

Li, R., Sun, F., Wang, W., Tang, J., Peng, H., Li, Z., Jiang, J., Zhan, T., Cai, L., and Lyu, J. (2025). "Effect of delignification on shrinking and swelling of poplar wood assessed using digital image correlation technique," *International Journal of Biological Macromolecules* 289, article 138851. DOI: 10.1016/j.ijbiomac.2024.138851

Li, Y., Cui, J., Shen, H., Liu, C., Wu, P., Qian, Z., Duan, Y., and Liu, D. (2022). "Useful spontaneous hygroelectricity from ambient air by ionic wood," *Nano Energy* 96, article 107065. DOI: 10.1016/j.nanoen.2022.107065

Liu, H., Han, Y., Zhang, X., Zhang, Y., Li, G., Lin, Z., Lei, Y., Chen, D., and Xue, L. (2025). "Graphene oxide sponge with gradient porosity for moisture-electric generator," *Journal of Bionic Engineering*. DOI: 10.1007/s42235-024-00641-0

Nguyen, Q. T., Tran, V. T., Vu, D. L., Le, C. D., Choi, W. M., and Ahn, K.-K. (2024). "Tribo-hygro-electric generator: Harnessing mechanical energy with liquid-infused porous cellulose for multiple sensing and DC power generation," *Nano Energy* 132, article 110353. DOI: 10.1016/j.nanoen.2024.110353

Shi, X., Wang, Z., Song, W., Hao, X., and Sun, D. (2025). "Development of far-infrared emitting functional wood via Co-doping of carbon nanotubes and nano-far-infrared ceramic powders for enhanced heating applications," *Industrial Crops and Products* 225, article 120491. DOI: 10.1016/j.indcrop.2025.120491

Tang, C., Yao, Y., Li, M., Wang, Y., Zhang, Y., Zhu, J., Wang, L., and Li, L. (2024). "A new polyvinyl alcohol lithium chloride hydrogel electrolyte: High Ionic conductivity and wide working temperature range," *Advanced Functional Materials* 24, article 17207. DOI: 10.1002/adfm.202417207

Wang, L., Xia, M., Li, L., Wu, Y., Cheng, Q., Xu, J., He, S., Liu, K., and Wang, D. (2024). "Sandwiched-structure fabric-based high-performance moisture-enabled electricity generators for the power supply of small electronics," *Journal of Colloid and Interface Science* 674, 1019-1024. DOI: 10.1016/j.jcis.2024.06.246

Zhang, H., Xu, F., Xu, L.,and Zheng, C. (2023). "The effect of delignification ratio on the PMMA occupation in poplar wood cell wall by the macro and micro comparative study," *Journal of Wood Science* 69, article 10. DOI: 10.1186/s10086-023-02082-5

Zhang, Z., Li, Z., Yao, L., Chang, S., and Wu, Y. (2024). "Development and performance evaluation of sunflower straw cellulose ether ecological sand-fixing material," *BioResources* 19(2), 2201-2215. DOI: 10.15376/biores.19.2.2201-2215

Zhou, L., Zhao, Z., Zhu, X., Liu, W., Tan, R., Li, Z., and Zhang, M. (2024) . "Characterization of water states and pore size distribution in Beijing poplar using nuclear magnetic resonance techniques," *Wood Material Science & Engineering* DOI: 10.1080/17480272.2024.2407981

Article submitted: December 22, 2024; Peer review completed: March 2, 2025; Revised version received and accepted: March 5, 2025; Published: March 17, 2025.
DOI: 10.15376/biores.20.2.3415-3423